ACS OMEGA

http://pubs.acs.org/journal/acsodf

Article

Nonanal Gas Sensors Using Porous Glass as a Reaction Field for Ammonia-Catalyzed Aldol Condensation

Masato Tsujiguchi,* Yasushi Kii, Takashi Aitoku, Masaru Iwao, and Yasuko Yamada Maruo

Cite This: *ACS Omega* 2023, 8, 7874−7882

Read Online

ACCESS | Metrics & More | Article Recommendations | Supporting Information

ABSTRACT: Transmittance in porous-glass gas sensors, which use aldol condensation of vanillin and nonanal as the detection mechanism for nonanal, decreases because of the production of carbonates by the sodium hydroxide catalyst. In this study, the reasons for the decrease in transmittance and the measures to overcome this issue were investigated. Alkali-resistant porous glass with nanoscale porosity and light transparency was employed as a reaction field in a nonanal gas sensor using ammonia-catalyzed aldol condensation. In this sensor, the gas detection mechanism involves measuring the changes in light absorption of vanillin arising from aldol condensation with nonanal. Furthermore, the problem of carbonate precipitation was solved with the use of ammonia as the catalyst, which effectively resolves the issue of reduced transmittance that occurs when a strong base, such as sodium hydroxide, is used as a catalyst. Additionally, the alkali-resistant glass exhibited solid acidity because of the incorporated SiO_2 and ZrO_2 additives, which supported approximately 50 times more ammonia on the glass surface for a longer duration than a conventional sensor. Moreover, the detection limit obtained from multiple measurements was approximately 0.66 ppm. In summary, the developed sensor exhibits a high sensitivity to minute changes in the absorbance spectrum because of the reduction in the baseline noise of the matrix transmittance.

INTRODUCTION

The progressive increase in both the global birthrate and aging populating has attracted increased interest in the development of new medical solutions, particularly in post-illness treatment and preventive medicine. Hence, new diagnostic methods for the early detection of diseases are currently being researched and developed. In the early 1970s, Pauling *et al.* reported that human-exhaled breath contained over 200 volatile organic compounds (VOCs);[1] subsequent studies have since identified over 3500 VOCs.[2] The composition of these VOCs has been widely adopted as an indicator of health status.[3−7] Thus, as diseases can be diagnosed from exhaled breath, non-invasive and rapid means of detecting VOCs could be very useful in the field of medical diagnosis.[6,7]

Cancers are a leading cause of death, among which lung cancer has a particularly high mortality rate. This is mainly because of the difficulty in detecting cancer disease markers in the early stages of illness. Thus, there is a growing need for convenient and sensitive detection of VOC markers for lung cancer. Several studies have compared the VOC concentration in the exhaled breath of lung cancer patients and healthy individuals;[8−13] significant differences in the concentration of nonanal have been reported.[11−13] Nonanal is an oxidative decomposition product of oleic acid;[14−17] it is generally accepted that as oleic acid oxidation progresses in lung cancer patients, the nonanal concentration in the exhaled air increases. Thus, nonanal can be a promising VOC marker for lung cancer diagnosis. Although several methods have been reported for sensing nonanal, including semiconductor sensing,[18] chemosensitive property variability,[19] and quartz crystal microbalance (QCM) measurements,[20,21] these methods demonstrate poor gas selectivity or sensitivity. Semiconductor gas sensors can detect nonanal at a level of several dozen parts per billion (ppb), but they must be loaded with a noble metal, such as platinum, to detect aliphatic hydrocarbon gas with high sensitivity and gas selectivity.[18] Chemosensitive and QCM sensors cannot detect sub-ppm levels of nonanal and do not show gas selectivity for aldehydes, which have structures similar to that of nonanal.[19−21]

We have previously reported a nonanal sensor utilizing porous glass and an aldol condensation reaction between nonanal and vanillin under alkaline conditions.[22] Because porous glass contains translucent nanopores, changes in the reactant color due to the chemical reactions occurring inside the pores can be easily detected.[22−24] In addition, porous glass has an inner-wall surface functionalized with silanol groups, which retains a thin water film because of its hydrophilicity. Thus, porous glass is a suitable nanoporous material for homogeneously supporting condensation reagents. Furthermore, the material has the potential to function as a reaction

Received: November 29, 2022
Accepted: January 19, 2023
Published: February 14, 2023

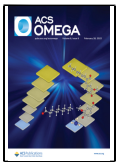

https://doi.org/10.1021/acsomega.2c07622
ACS Omega 2023, 8, 7874−7882

field for trace-level gas detection reactions. We therefore proposed to use it as a reagent carrier and reaction field for gas sensors, using the change in the absorption spectra of the condensation reagents as the detection mechanism. For this purpose, we had prepared alkali-resistant porous glass using sodium hydroxide as an alkali catalyst. The limit of detection (LOD) was found to be in the order of 10^2 ppb; however, the gas sensor exhibited a low transmittance.[22] Nevertheless, the sensor was able to detect changes in absorbance caused by the aldol condensation of vanillin and nonanal within the inner surfaces of the porous glass. However, detecting minute changes in absorbance becomes challenging when the transmittance of the porous glass decreases. In addition, the resulting increase in the lower LOD value becomes disadvantageous.

To address these shortcomings, we investigated the factor responsible for decreasing the transmittance of sodium hydroxide-loaded porous glass gas sensors. To achieve this, we employed ammonia as an alternative catalyst and compared its performance to that of the hydroxide-loaded sensor. Through the findings discussed herein, we suggest measures that may overcome the detection issues in nonanal gas sensors.

EXPERIMENTAL SECTION

Porous Glass Preparation. Porous glass was prepared by a phase-separation method, as shown in Figure S1.[22] Soda borosilicate glass was subjected to heat treatment at the glass transition temperature (or higher) and separated into silica and soda boron oxide phases. The soda boron oxide phase was leached with an acid solution to produce pores, whereas the silica phase was not leached, forming a skeleton.[26,27]

In addition to the conventional borosilicate components for porous glass (SiO_2, B_2O_3, and Na_2O),[26,27] raw materials included K_2O, Al_2O_3, CaO, P_2O_5, TiO_2, and ZrO_2. In particular, ZrO_2 was added to improve the alkali resistance of the glass. The materials were placed in a platinum crucible and melted at 1773 K. The molten glass was then rolled, molded on an iron plate to form a plate, and gradually cooled. The glass sample was processed to a size of 5 × 5 × 0.5 mm and subjected to a phase heat treatment at 968 K. The fractional glass sample was then leached with 1 mol/L aqueous nitric acid.

The glass sample was further leached with 1.5 mol/L aqueous sulfuric acid followed by 0.5 mol/L aqueous sodium hydroxide and then washed with ion-exchanged water.

Porous Glass Evaluation. Scanning electron microscopy (SEM) was performed using a field emission scanning electron microscope (SU-8820, Hitachi, Japan) at an accelerating voltage of 1.6 kV. The ultraviolet−visible (UV−Vis) spectra of the porous glass samples were obtained using a spectrophotometer (UH-4150, Hitachi High-Tech, Japan) in a wavelength range of 300−800 nm. The pore-size distribution of the porous glass was determined using a nitrogen adsorbent and a surface/pore-size analyzer (Quadrasorb SI, Anton Paar, Austria).

Estimation of Changes in the Absorption Spectra. For the sodium hydroxide-loaded and ammonia-loaded porous glass samples, the relationship between their absorption spectra and the elapsed time after base treatment was estimated. For these spectra, the samples were measured between 300 and 800 nm after exposure time intervals of 0.05 (3 min), 1, 3, and 6 h. The hydroxide-loaded sample was also subjected to X-ray diffraction (XRD) and cross-sectional SEM observations after each time interval. The ammonia-loaded sample was subjected to XRD measurements only after the 6 h interval, in addition to the SEM observation. The XRD analysis was performed at 2θ = 35−40° using a powder X-ray diffractometer (Smart-Lab, Rigaku, Japan).

Solution System Evaluation. A solution system was tested to investigate the spectra of vanillin, nonanal, and the reaction products. Vanillin ($C_8H_8O_3$, 0.5 g, Wako special grade, FUJIFILM Wako Pure Chemical Corporation, Japan) was dissolved in a solution containing 6.5 mL of ion-exchanged water and 33.5 mL of aqueous ammonia (30 wt %, Wako special grade, FUJIFILM Wako Pure Chemical Corporation, Japan). Subsequently, 2.7 mmol/L of an ethanol solution of nonanal was prepared using pure ethanol (C_2H_5OH, Wako special grade, FUJIFILM Wako Pure Chemical Corporation) and nonanal ($CH_3(CH_2)_7CHO$, Wako first grade, FUJIFILM Wako Pure Chemical Corporation). Then, 1 mL of an ethanol solution of nonanal was added to the vanillin-ammonia solution. The solution was then transferred to an Erlenmeyer flask, sealed, and heated in a water bath at 373 K for 1 h; this solution was then used for the UV−Vis spectroscopic analysis. The measurement range was 350−700 nm. Nonanal and vanillin were dissolved in acetonitrile and water, respectively, to obtain their reference absorption spectra.

Evaluation of the Ammonia-Supporting Ability and Nonanal-Adsorbing Capacity of Porous Glass. The amount of ammonia supported on the sensor chip was measured by thermal desorption spectrometry (TDS). The sensor chip sample was placed in a quartz glass container, which was filled with helium gas and externally heated from 323 to 773 K. The gas released from the glass container during the temperature increase was analyzed using a quadrupole mass spectrometer (M-101QA-TDM, Canon-Anelva, Japan). The amount of ammonia on the sensor was evaluated using ion currents with a mass-to-charge ratio of 17. The spectrometer ion current was calibrated to the expected value by subtracting the current corresponding to the fragments from water. The spectrometer ion current was obtained at standard temperature and pressure (STP; 273 K, 1 atm). The amount of ammonia supported per unit surface area in the pores of the porous glass was expressed by converting it into a gas at STP.

Vanillin (0.1 g) was dissolved in 10 mL of deionized water to prepare a 1 wt % aqueous solution, which was then mixed with 5 mL of aqueous ammonia (30 wt %, Kanto Chemical, special grade, Kanto Chemical Co., Inc., Japan). Subsequently, the porous glass was immersed in 20 μL of the mixed solution using a microdispenser (Dialamatic 3-000-250, Drummond Scientific, USA). The sample was then dried at 298 K for 24 h under vacuum to obtain a sensor chip. The absorption spectrum and microstructure of the sensor chip were analyzed by UV−Vis spectroscopy and SEM, respectively.

The nonanal-adsorbing capacity of the porous glass was also evaluated using 1 L atmosphere. At first, a 50-L Tedlar bag (1-2711-08, Asone, Japan) was filled with nitrogen (Industrial Grade, Iwatani, Japan). Subsequently, 0.125 mL of nonanal was diluted to 50 mL with ethanol; 40 μL of this solution was then placed in the Tedlar bag to achieve a nonanal atmosphere of 0.28 ppm. Then, 1 L of atmosphere was adjusted by subdividing 50 L of nonanal atmosphere of 0.28 ppm as described above, and the porous glass was in a polytetrafluoroethylene (PTFE) mesh film was hung in the 1 L Tedlar bag. After a predetermined time (every 30 min), the sensor was removed from the Tedlar bag, and the nonanal concentration

https://doi.org/10.1021/acsomega.2c07622
ACS Omega 2023, 8, 7874−7882

in the bag was measured using a sensor gas chromatograph (SGVA-P3-A, Nissha FIS Inc., Japan).

Nonanal Sensing Test. The nonanal-sensing ability of the prepared sensor was also investigated (Figure 1). 50 liter

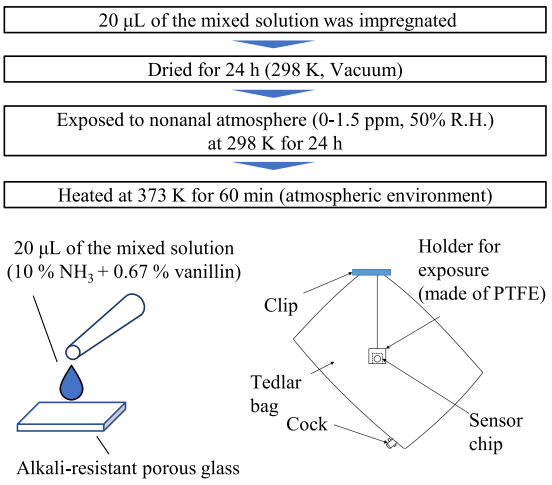

Figure 1. Illustration of a nonanal sensor chip preparation process and a subsequent nonanal sensing test.

Tedlar bags were filled with nitrogen in the same manner as described previously. Various concentrations of nonanal (0, 250, 500, and 750 μL) were diluted to 50 mL with ethanol. Each resulting nonanal solution (40 μL) was placed in a Tedlar bag to achieve a nonanal atmosphere of 0, 0.5, 1.0, or 1.5 ppm. After this, 575 mL of deionized water was placed in the Tedlar bag to achieve a relative humidity of 50%. For each nonanal concentration, a sensor chip was wrapped in a PTFE mesh bag and hung with Teflon thread inside the Tedlar bag for 24 h. This exposure time was selected because the sensing mechanism is based on accumulation of nonanal inside the sensor chip;[22] in our previous study, it was confirmed that the sensor sensitivity increased until 24 h. After this period, the sensor was removed from the Tedlar bag and heated at 373 K for 1 h on a hot plate to promote the aldol condensation reaction. The absorption spectrum of the sensor chip was then obtained using UV−Vis spectroscopy.

RESULTS AND DISCUSSION

Evaluation of Alkali-Resistant Porous Glass Sample. The appearance and microstructure of the obtained glass sample, its transmission spectrum, and the pore distribution are shown in Figure 2. The exterior photograph (Figure 2a) shows that the sensor is translucent, while the transmission spectrum (Figure 2c) confirms that the sensor transmittance is between 10% and 90% in the wavelength range of visible light (400−800 nm). In particular, the transmittance at approximately 420 nm, where the absorption of vanillin is expected,[22] is approximately 10%. At shorter wavelengths, the transmittance decreases because of Rayleigh scattering in the porous structure.[28] Notably, if the pore size decreases, the transmittance increases; however, it then becomes difficult for the gas to diffuse into the pores. The calculated mean free path of nonanal was 9 nm according to the Maxwell−Boltzmann approximation.[22] If the pore size is reduced further to increase the transmittance, Knudsen diffusion occurs, which causes the rate of gas diffusion into the pores to become very low as the mean free path and pore size become equivalent.[29]

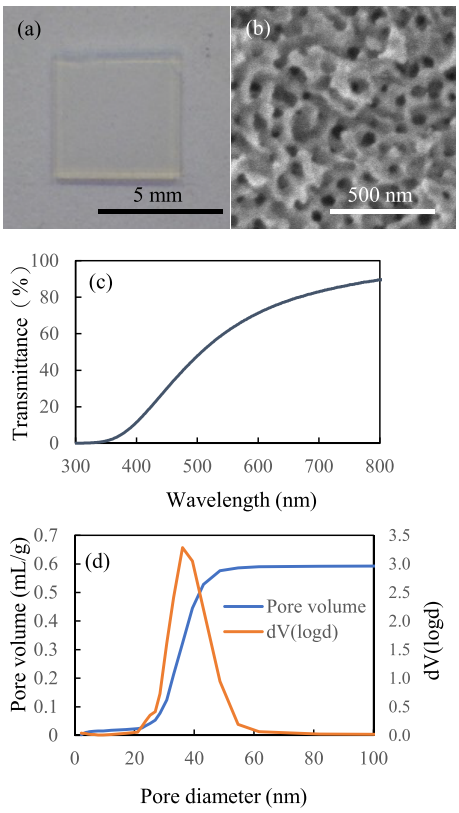

Figure 2. (a) Exterior photograph and (b) SEM image of an alkali-resistant porous glass sample; (c) UV−Vis transmittance spectrum of the sample; (d) pore-size distribution of the sample as determined by a nitrogen adsorption method.

An SEM photograph of the microstructure (Figure 2b) shows a porous structure arising from the spinodal phase. In the pore-size distribution determined by the nitrogen adsorption method (Figure 2d), the median pore diameter was found to be approximately 35 nm, and 80% of the pores were between 20 and 50 nm in size. SEM observations also confirmed this distribution range. Therefore, the obtained pore sizes are sufficiently large for nonanal gas diffusion when considering the mean free path. Consequently, the resulting porous glass is a suitable material for a gas sensor matrix that combines desirable light transmission and gas diffusibility.

Evaluation of the Absorption Changes upon Sodium Hydroxide and Ammonia Treatment. A porous glass treated with sodium hydroxide exhibits a considerably reduced transmittance compared to a non-treated glass, as reported in a previous study.[22] Hence, the sodium hydroxide-loaded porous glass sample was subjected to absorption, cross-sectional SEM, and XRD measurements at exposure to an air atmosphere at designated time intervals to investigate the factor responsible for the decreased transmittance. These results are presented in Figure 3.

After vacuum drying, the sodium hydroxide-loaded glass exhibited an increase in absorbance with exposure time (Figure 3a). Furthermore, the intensity of the diffraction peak corresponding to sodium carbonate also increased with exposure time (Figure 3b). This result is attributed to the reaction of sodium hydroxide with carbon dioxide from the air inside the pores, which generates sodium carbonate.[30] In addition, the cross-sectional SEM observation confirmed the precipitation of coarse particles within the porous glass sample

https://doi.org/10.1021/acsomega.2c07622
ACS Omega 2023, 8, 7874−7882

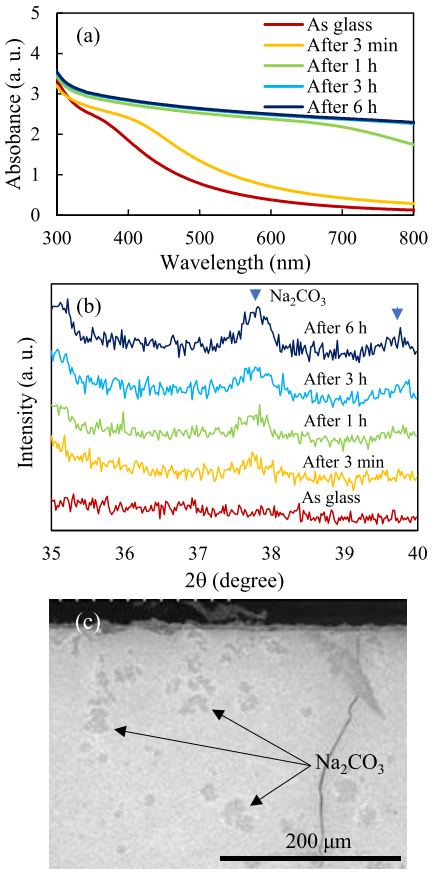

Figure 3. (a) UV−Vis absorption spectra and (b) XRD patterns of sodium hydroxide-loaded glass after several time intervals of NaOH exposure; (c) cross-sectional SEM image of the sodium hydroxide-loaded porous glass.

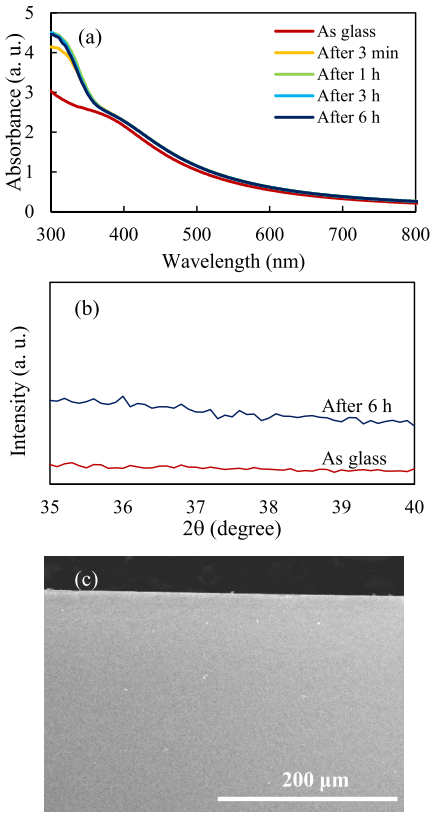

Figure 4. (a) UV−Vis absorption spectra and (b) XRD patterns of ammonia-supported glass after several time intervals of ammonia exposure; (c) cross-sectional SEM image of the ammonia-loaded porous glass.

after an elapsed time period post drying (Figure 3c), which can be attributed to the growth of sodium carbonate crystals. From these results, it can be concluded that the sodium hydroxide treatment of the porous glass generates coarse particles of sodium carbonate within the pores; these particles then scatter the incident light, which decreases the sensor transmittance. As the transmittance of the porous glass decreases (and the absorbance increases), the sensor sensitivity to minute absorbance changes during the aldol condensation reaction also decreases. Measures to prevent this deterioration in transmittance were therefore required.

As an alternative, a porous glass was produced utilizing weakly alkaline ammonia as the alkali catalyst instead of the strongly alkaline sodium hydroxide. Figure 4a shows the absorbance changes of the ammonia-loaded porous glass with exposure time. After vacuum drying, the absorbance at wavelengths of above 370 nm barely changed with each time interval. In addition, crystal-derived diffraction peaks were not observed after the longest exposure period (Figure 4b). Furthermore, the cross-sectional SEM image (Figure 4c) revealed that the ammonia-loaded porous glass differs considerably from the sodium hydroxide-loaded sample; no precipitation of coarse particulate crystals can be observed within the material. The above results therefore suggest that the transmittance of the ammonia-loaded porous glass is unchanged with exposure time because of the lack of precipitation of coarse carbonate crystal particles.

Evaluation of the Solution System Reaction between Nonanal and Vanillin Using an Ammonia Catalyst. Ammonia was used in a solution system to confirm its role as a catalyst in the reaction between nonanal and vanillin, which was used as a nonanal-detecting reagent in our previous study.[22] The changes in the absorbance spectra of different reagent mixtures due to heating (when applied to promote the aldol condensation reaction) are illustrated in Figure 5. When only vanillin and ammonia were mixed as a control system, an absorbance of approximately 0.003 was observed at 500 nm (Figure 5a); this did not change notably (0.006 at 500 nm) when ethanol was added to the mixed solution. However, the absorbance changed after the solution was heated to 373 K for 1 h (0.086 at 500 nm); this is caused by the formation of side products from the reaction of vanillin and ammonia, owing to the high reactivity of the hydroxy group in vanillin at elevated temperatures (Figure S2) and the possible spontaneous reaction of ammonia with the aldehyde group.[31] While such a change is likely to decrease the sensor sensitivity, the subsequently measured calibration curve (Figure 10) shows that the transmittance was still higher than that of the sodium hydroxide-loaded sensor by an order of magnitude. When diluted nonanal was added to the vanillin/ammonia system, the absorbance remained approximately constant before heating (Figure 5b); however, the change after heating (0.14 at 500 nm) was notably greater than that observed for the control solution (as seen in Figure 5c). This additional absorbance increase across the studied wavelength range indicates a formation of a product from the reaction between nonanal and vanillin.

https://doi.org/10.1021/acsomega.2c07622
ACS Omega 2023, 8, 7874−7882

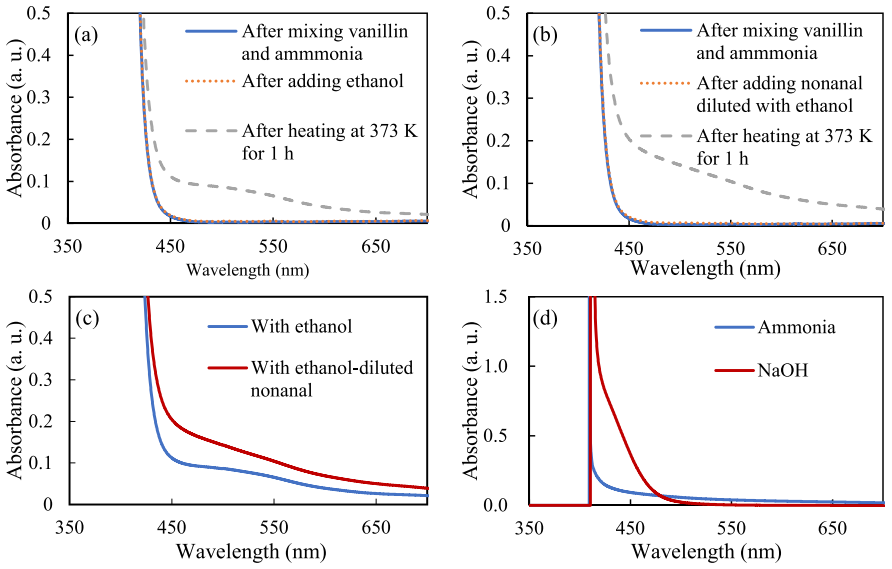

Figure 5. Absorption spectra of solution systems before and after heating at 373 K for 1 h: (a) vanillin and ammonia mixed with ethanol, and (b) vanillin and ammonia mixed with ethanol-diluted nonanal; comparisons of the post-reaction absorbance spectra of (c) the control and nonanal-mixed ammonia-catalyzed solutions and (d) the nonanal mixed ammonia- and sodium hydroxide-catalyzed solutions.

Figure 5d illustrates the difference between the absorption spectra of the reaction product mixture when either sodium hydroxide or ammonia was used as the catalyst. While the sodium hydroxide-catalyzed reaction mixture showed a large absorbance with a narrow range of approximately 400−480 nm, the ammonia-catalyzed mixture showed a larger absorbance across a broader wavelength band of approximately 480−700 nm. This may be attributed to the products formed from the additional side reactions of ammonia with vanillin.

Ammonia-Supporting Ability and Nonanal-Adsorbing Capacity of Porous Glass. Next, the ammonia-supporting ability of the porous glass was evaluated. Figure 6 shows the TDS profile of ammonia released from a gas sensor element carrying ammonia and vanillin. Two peaks appear at 423 and 543 K; these positions are identical to those observed previously in TDS profiles of ammonia released from solid acidic porous materials such as zeolite.[32] The peak at 423 K is caused by the desorption of the physically adsorbed ammonia, whereas the peak at 543 K arises from the desorption of ammonia from the acidic sites in the porous structure. These results suggest that ammonia adsorbs to the glass by two means: weak physisorption and acid−base interactions.

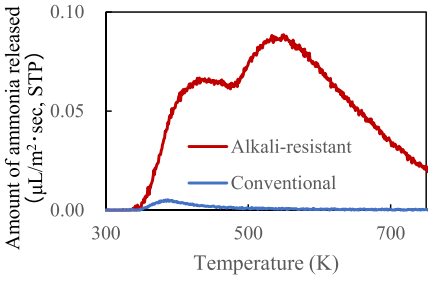

Figure 6. Thermal desorption spectra of ammonia released from alkali-resistant porous glass and conventional porous glass exposed to a mixed ammonia/vanillin solution.

The ammonia TDS profile of a control sample in which ammonia and vanillin were supported in a conventional porous glass product[26,27] is also shown in Figure 6. Only a small peak in the spectrum can be observed at a peak temperature of 383 K. Thus, as the conventional product does not contain acidic sites, only the physically adsorbed ammonia is retained in the pores.

In addition, when the amount of adsorbed ammonia (obtained from the peak area by integrating the TDS curve) was compared between the two samples, the treated product was found to contain approximately 50 times more ammonia than the conventional product. This finding suggests that the treated product retains more ammonia because of the acidic sites in its pores. It has been reported that the composite oxides of SiO_2 and ZrO_2, which are the main components of porous glass, have high acidity.[33,34] Similarly, the acidity of SiO_2 was strong, even in porous glasses containing SiO_2 and ZrO_2, and the peak splits into two as ammonia adsorption increases to the acid point, thereby indicating an increase in the retention amount of ammonia.

In addition, the evaluation results of the nonanal-adsorbing performance of the porous glass are shown in Figure 7. The evaluation was performed on both pristine and ammonia-loaded porous glass samples. The nonanal adsorption rate was larger in the pristine glass compared to that of the ammonia-supported sample, owing to the strongly acidic pore surfaces in the pristine glass. It is assumed that the carbonyl groups in

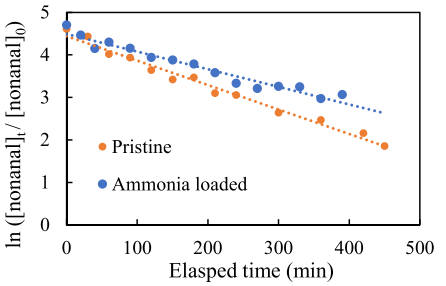

Figure 7. Amount of nonanal adsorbed on pristine and ammonia-loaded alkali-resistant porous glasses.

https://doi.org/10.1021/acsomega.2c07622
ACS Omega 2023, 8, 7874−7882

nonanal interacted with the acidic pore surfaces; as the carbonyl carbon is positively charged due to the polarization induced by oxygen,[35] these groups should therefore have a strong affinity to the negatively charged acidic sites under aqueous conditions. Conversely, when ammonia was supported on the pores, the surface acidity of the pores was neutralized by the basic ammonia, thus weakening the overall acidity in the material. These modified sites should therefore become positively charged in aqueous conditions, thus reducing the overall negative charge on the glass surface and weakening the carbonyl interactions.

Nonanal Gas Detection Test and Sensor Calibration Curve. Figure 8 shows three absorption spectra of the porous glass sensor chip: the sensor chip before loading, the sensor with vanillin and ammonia supported in the pores, and the sensor after exposure to nonanal with subsequent heating for 1 h. Nonanal concentration, exposure time, and heating conditions were 1 ppm, 24 h, and 373 K, respectively. Notably, the absorption of the original porous glass increases at lower wavelengths owing to Rayleigh scattering caused by the microstructure.[29] When the gas detectors were loaded with ammonia and vanillin, the absorption remained unchanged over 450 nm; however, the absorption below 450 nm increased owing to the absorption of light by the supported vanillin. This conclusion is supported by the previously confirmed fact that crystal precipitation does not occur in the sensor when exposed to ammonia. These spectral changes therefore demonstrate the formation of a gas detection layer within the porous structure. After exposure to nonanal and heating, the sensor absorption below 450 nm increased, suggesting the occurrence of aldol condensation between vanillin and nonanal inside the sensor pores. This result also supports the observations seen on the solution system experiments.

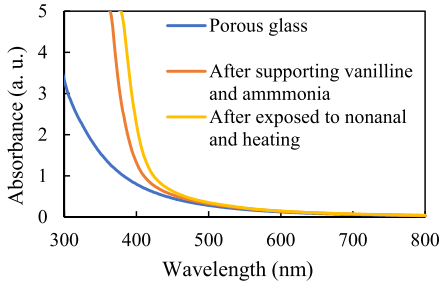

Figure 8. Absorption spectra (300−800 nm) of the gas sensor chip before loading, after vanillin and ammonia loading, and after exposure to 1 ppm nonanal gas for 24 h followed by subsequent heating (373 K, 1 h).

Figure 9 illustrates the visual appearance of the sensor chips before and after the nonanal gas exposure and heating process. The vanillin-loaded sensor chip became slightly yellow due to the absorbance of vanillin at below 400 nm. The color then intensified after nonanal gas exposure and heating, which is in accordance with the absorption spectrum change. The color also darkened after zero nonanal gas exposure and heating, which can be attributed to the side reaction of vanillin and ammonia at the heating stage. However, the color change in the sensor chip exposed to nonanal was still distinct enough to be identified.

Figure 10 illustrates the relationship between the nonanal concentration and the change in sensor absorbance at 420 nm. The amount of aldol condensation, which determines the absorbance change, depends on the amount of vanillin and nonanal gas accumulated on the chip. The amount of nonanal gas accumulated on the sensor chip was proportional to the nonanal concentration in the atmosphere and exposure time.[22] Therefore, the amount of aldol condensation is proportional to the amount of vanillin, nonanal concentration of the atmosphere, and exposure time. In this study, the amount of vanillin and exposure time were constant. Thus, the absorbance shift linearly increased with the nonanal concentration. The proportionality constant can be obtained from the slope in Figure 10. A large constant was obtained because of the large specific surface area of the glass, which leads to an increase in its adsorption capacity

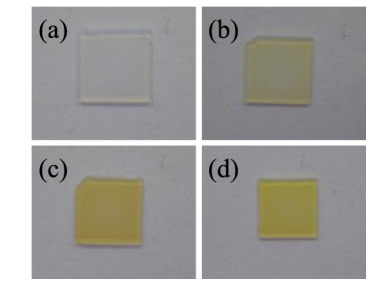

Figure 9. Photographs of (a) untreated alkali-resistant porous glass, (b) nonanal sensor chip after vanillin and ammonia loading, and nonanal sensor after exposure to (c) 0 or (d) 1 ppm nonanal with subsequent heating.

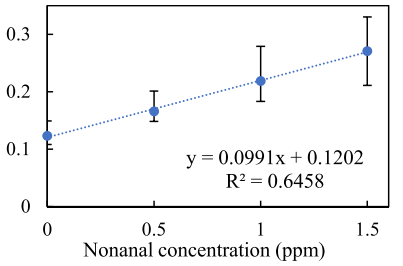

Figure 10. Calibration curve illustrating the relationship between nonanal concentration and the change in absorbance at 420 nm.

The absorbance change was evaluated at 420 nm because absorbances obtained at wavelengths less than 420 nm increase sharply owing to the absorbance of vanillin. If a wavelength less than 420 nm is chosen, the error of subtraction becomes relatively large; however, if a wavelength greater than 420 nm is chosen, the change in absorbance would decrease significantly because the absorbance decreases with increasing wavelength.

The sensitivity of the developed sensor was also analyzed. The obtained calibration curve shows a one-to-one correspondence in a concentration range of 0.1−1.5 ppm; thus, the sensor can measure sub-ppm nonanal concentrations. The standard deviation and coefficient of variation obtained from multiple blank measurements were 0.022 and 18%, respectively. The three-sigma value was 0.066, which corresponds to the LOD of the absorbance change after considering the experimental variation. The absorbance change per unit of concentration (ppm) was approximately 0.1; thus, an absorbance change of 0.066 is equivalent to 0.66 ppm of nonanal. Consequently, the LOD of the developed nonanal sensor is 0.66 ppm. This sensitivity is comparable to those obtained with other types of gas sensors, which range between several dozen ppb to several ppm.[17−20,36,37]

https://doi.org/10.1021/acsomega.2c07622
ACS Omega 2023, 8, 7874−7882

The limit of quantification (LOQ) of the sensor was determined from the ten-sigma value and gradient of the calibration curve, where LOQ = ten-sigma/gradient.[38] For the developed sensor, the ten-sigma value was 0.22, while the curve gradient was 0.1, giving the LOQ of 2.2 ppm. However, this value is insufficient for diagnosing lung cancer, which requires a sensitivity in the order of several ppb.[11−13]

In this study, we focused on increasing the transmittance of the sensor chip because the accuracy of an absorbance measurement increases with transmittance. The absorption measurement resolution of spectrometers is generally less than or equal to 0.005 a.u. when the transmittance is higher than 10%. In this study, it was confirmed that transmittance through the sensor chip can exceed 10% when ammonia is used as the catalyst. An absorbance change of 0.005 is equivalent to a 50-ppb nonanal concentration change in the calibration curve; considering that the developed sensor variation is related to variations in the porous structure and thus the amount of loaded detection reagents, this phenomenon indicates that the sensor may potentially achieve an LOD of approximately 50 ppb if the sensor variability is controlled or suppressed. Thus, the developed sensor is potentially suitable for gas detection over a wide nonanal concentration range of between 50 ppb and 1.5 ppm.

Furthermore, we investigated the sensors at an atmospheric humidity of approximately 50%. Notably, the sensitivity of a porous glass sensor increases with increasing humidity, which is because the water layer inside the porous structure becomes more stable.[25,39] This is a positive attribute of this sensor in comparison to semiconductor sensors, which become less sensitive with increasing humidity. Variations due to humidity changes can also be corrected by in situ monitoring and subsequent sensitivity correction; for example, using automated software processes.

The selectivity of the sensor is another important aspect to consider. Exhaled breath contains aldehydes; thus, the operational sensor must be able to distinguish between nonanal and other aldehyde gases, especially C_8 and C_{10} aliphatic aldehydes, which are similar in size to nonanal. The sensor was therefore evaluated for its sensitivity to octanal ($C_8H_{16}O$) and decanal ($C_{10}H_{20}O$). It was found that increasing the number of carbons in the aldehyde backbone increases the sensitivity because the molecular boiling point increases with increasing molecular weight; the sensor was therefore more sensitive to decanal than octanal. Thus, there is scope for future work to be conducted by investigating the differentiation of gases by the sensor as a function of the pore size or other parameters. An additional limitation of the developed sensor is the irreversible nature of the sensing mechanism, whereas semiconductor gas sensors can be used repeatedly.

Moreover, when considering the future application of this sensor type toward point-of-care diagnostic devices, it would be preferable that the porous glass matrix be incorporated into a metal framework that can be easily heated by a miniature heating device. LEDs and optical detectors may also enable the measurement of an adsorption change at a specified wavelength.[24,40] To enable the practical use of this sensor type, supporting device technologies will need to be developed.

CONCLUSIONS

In this study, we used ammonia instead of sodium hydroxide as a catalyst in a porous glass gas sensor for the detection of nonanal. This prevented the deterioration in transmittance that was observed previously in sodium hydroxide-loaded sensors and was subsequently found to be caused by the formation of carbonate deposits in the sensor. In a model solution system, when ammonia was used to catalyze the aldol condensation of vanillin with nonanal, the absorbance changed in response to the presence or absence of nonanal. Because ammonia tends to volatilize, the retention performance of the developed porous glass was greater than that of the conventional porous glass, owing to the former's higher surface acidity. A comparison of the retained amount of ammonia revealed that the developed product contained 50 times more ammonia than the conventional product. When the sensor was subsequently tested for the detection of gaseous nonanal, specific absorption changes were observed in accordance with the solution system experiments. The resulting calibration curve indicated a linear relationship between nonanal concentration and absorbance, confirming the feasibility of the sensor for quantitative detection, with the LOD found to be 0.66 ppm. Moreover, when ammonia was used as the catalyst instead of sodium hydroxide, the transmittance of the sensor chip was improved, leading to the detection of minute absorbance changes. Notably, high sensitivity may be achieved when the sensor variation is suppressed. This new porous glass sensor therefore provides a practical sensing mechanism for nonanal detection that utilizes ammonia-catalyzed aldol condensation. By utilizing the properties of the pore surfaces, we demonstrated that ammonia can be stably and homogeneously used as a catalyst in nanoscale environments. Thus, porous glass materials can be used as sensing platforms that can provide nanoscale reaction fields and catalytic activity owing to their significant surface properties. Such materials are promising candidates for sensing materials in future point-of-care diagnostic devices. Future research should focus on investigating the ability of the sensor to differentiate gases according to pore size or other properties.

ASSOCIATED CONTENT

Supporting Information

The Supporting Information is available free of charge at https://pubs.acs.org/doi/10.1021/acsomega.2c07622.

Schematic of the preparation process of the alkali-resistant porous glass; chemical structures of nonanal and vanillin; reaction scheme of the aldol condensation reaction between vanillin and nonanal (PDF)

AUTHOR INFORMATION

Corresponding Author

Masato Tsujiguchi − *Development Division, Research and Development Group, Nippon Electric Glass Co., Ltd., Otsu, Shiga 520-8639, Japan;* orcid.org/0000-0002-7629-7838; Email: mtsujiguchi@neg.co.jp

Authors

Yasushi Kii − *Evaluation Division, Research and Development Group, Nippon Electric Glass Co., Ltd., Otsu, Shiga 520-8639, Japan*

Takashi Aitoku − *Development Division, Research and Development Group, Nippon Electric Glass Co., Ltd., Otsu, Shiga 520-8639, Japan*

https://doi.org/10.1021/acsomega.2c07622
ACS Omega 2023, 8, 7874−7882

Masaru Iwao − *Development Division, Research and Development Group, Nippon Electric Glass Co., Ltd., Otsu, Shiga 520-8639, Japan*
Yasuko Yamada Maruo − *Department of Applied Chemistry and Environment, Faculty of Engineering, Tohoku Institute of Technology, Sendai 982-8577, Japan*

Complete contact information is available at: https://pubs.acs.org/10.1021/acsomega.2c07622

Author Contributions

M.T. conceived the project, performed the experiments, and wrote the manuscript. Y.K. significantly contributed to the TDS measurements. T.A. contributed to the porous glass synthesis. M.I. and Y.Y.M. contributed to the experiments and supervised the work. All the authors have approved the final version of the manuscript.

Funding

This research did not receive any specific grants from funding agencies in the public, commercial, or not-for-profit sectors.

Notes

The authors declare no competing financial interest.

■ ACKNOWLEDGMENTS

The authors thank Noriaki Masuda of Nippon Electric Glass Co., Ltd., for his support and useful discussions regarding this study. The authors also thank Naoki Toyofuku of Nippon Electric Glass Co., Ltd., for his support in the XRD measurements. The authors also thank Yuki Sato of the Tohoku Institute of Technology for her support in the solution system and nonanal sensing tests.

■ ABBREVIATIONS

LOD, limit of detection; PTFE, polytetrafluoroethylene; SEM, scanning electron microscopy; TDS, thermal desorption spectrometry; UV−Vis, ultraviolet−visible; VOC, volatile organic compound; XRD, X-ray diffraction

■ REFERENCES

(1) Pauling, L.; Robinson, A. B.; Teranishi, R.; Cary, P. Quantitative Analysis of Urine Vapor and Breath by Gas-Liquid Partition Chromatography. *Proc. Natl. Acad. Sci. U. S. A.* **1971**, *68*, 2374−2376.
(2) Popov, T. A. Human exhaled breath analysis. *Ann. Allergy Asthma Immunol.* **2011**, *106*, 451−456.
(3) Sinues, M.-L. P.; Kohler, M.; Zenobi, R. Human breath analysis may support the existence of individual metabolic phenotypes. *PLoS One* **2013**, *8*, No. e59909.
(4) Francesco, F. D.; Fuoco, R.; Trivella, M. G.; Ceccarini, A. Breath analysis: trends in techniques and clinical applications. *Microchem. J.* **2005**, *79*, 405−410.
(5) Righettoni, M.; Amann, A.; Pratsinis, S. E. Breath analysis by nanostructured metal oxides as chemo-resistive gas sensors. *Mater. Today* **2015**, *18*, 163−171.
(6) Buszewski, B.; Kęsy, M.; Ligor, T.; Amann, A. Human exhaled air analytics: biomarkers of diseases. *Biomed. Chromatogr.* **2007**, *21*, 553−566.
(7) Phillips, M.; Beatty, J. D.; Cataneo, R. N.; Huston, J.; Kaplan, P. D.; Lalisang, R. I.; Lambin, P.; Lobbes, M. B. I.; Mundada, M.; Pappas, N.; Patel, U. Rapid point-of-care breath test for biomarkers of breast cancer and abnormal mammograms. *PLoS One* **2014**, *9*, No. e90226.
(8) The National Lung Screening Trial Research Team. Reduced lung-cancer mortality with low-dose computed tomographic screening. *N. Engl. J. Med.* **2011**, *365*, 395−409.
(9) Ratiu, A. I.; Ligor, T.; Bocos-Bintintan, V.; Mayhew, A. C.; Buszewsli, B. Volatile organic compounds in exhaled breath as fingerprints of lung cancer, asthma and COPD. *J. Clin. Med.* **2020**, *10*, 32.
(10) Campanella, A.; Summa, D. S.; Tommasi, S. Exhaled breath condensate biomarkers for lung cancer. *J. Breath Res.* **2019**, *13*, No. 044002.
(11) Fuchs, P.; Loeseken, C.; Schubert, J. K.; Miekisch, W. Breath gas aldehydes as biomarkers of lung cancer. *Int. J. Cancer* **2010**, *126*, 2663−2670.
(12) Das, S.; Pal, M. Non-invasive monitoring of human health by exhaled breath analysis: a comprehensive review. *J. Electrochem. Soc.* **2020**, *167*, No. 037562.
(13) Zhou, X.; Xue, Z.; Chen, X.; Huang, C.; Bai, W.; Lu, Z.; Wang, T. Nanomaterial-based gas sensors used for breath diagnosis. *J. Mater. Chem. B* **2020**, *8*, 3231−3248.
(14) Mochalski, P.; King, J.; Unterkofler, K.; Hinterhuber, H.; Amann, A. Emission rates of selected volatile organic compounds from skin of healthy volunteers. *J. Chromatogr., B* **2014**, *959*, 62−70.
(15) Haze, S.; Gozu, Y.; Nakamura, S.; Kohno, Y.; Sawano, K.; Ohta, H.; Yamazaki, K. 2-Nonenal newly found in human body odor tends to increase with aging. *J. Invest. Dermatol.* **2001**, *116*, 520−524.
(16) Fujisaki, M.; Endo, Y.; Fujimoto, K. Retardation of volatile aldehyde formation in the exhaust of frying oil by heating under low oxygen atmospheres. *J. Am. Oil Chem. Soc.* **2002**, *79*, 909−914.
(17) Mochalski, P.; Unterkofler, K.; Teschl, G.; Amann, A. Potential of volatile organic compounds as markers of entrapped humans for use in urban search-and-rescue operations. *TrAC Trends Anal. Chem.* **2015**, *68*, 88−106.
(18) Itoh, T.; Nakashima, T.; Akamatsu, T.; Izu, N.; Shin, W. Nonanal gas sensing properties of platinum, palladium, and gold-loaded tin oxide VOCs sensors. *Sens. Actuators, B* **2013**, *187*, 135−141.
(19) Daneshkhah, A.; Vij, S.; Siegel, A. P.; Agarwal, M. Polyetherimide/carbon black composite sensors demonstrate selective detection of medium-chain aldehydes including nonanal. *Chem. Eng. J.* **2020**, *383*, No. 123104.
(20) Jha, S. K.; Hayashi, K. Polyacrylic acid polymer and aldehydes template molecule based MIPs coated QCM sensors for detection of pattern aldehydes in body odor. *Sens. Actuators, B* **2015**, *206*, 471−487.
(21) Wasilewski, T.; Szulczyński, B.; Wojciechowski, M.; Kamysz, W.; Gębicki, J. Determination of long-chain aldehydes using a novel quartz crystal microbalance sensor based on a biomimetic peptide. *Microchem. J.* **2020**, *154*, No. 104509.
(22) Tsujiguchi, M.; Aitoku, T.; Takase, H.; Maruo, Y. Y. Nonanal sensor fabrication using aldol condensation reaction inside alkali-resistant porous glass. *IEEE Sens. J.* **2021**, *21*, 8868−8877.
(23) Maruo, Y. Y.; Nakamura, J.; Uchiyama, M.; Higuchi, M.; Izumi, K. Development of formaldehyde sensing element using porous glass impregnated with Schiff's reagent. *Sens. Actuators, B* **2008**, *129*, 544−550.
(24) Maruo, Y. Y.; Nakamura, J. Portable formaldehyde monitoring device using porous glass sensor and its applications in indoor air quality studies. *Anal. Chim. Acta* **2011**, *702*, 247−253.
(25) Maruo, Y. Y.; Tachibana, K.; Suzuki, Y.; Shinomi, K. Development of an analytical chip for detecting acetone using a reaction between acetone and 2,4-dinitrophenylhidrazine in a porous glass. *Microchem. J.* **2018**, *141*, 377−381.
(26) Porter, H. H.; Emery, N. M. Treated Borosilicate Glass; US Patent 2, 106, 744, 1938.
(27) Enke, D.; Janowski, F.; Schwieger, W. Porous glasses in the 21st century−−a short review. *Microporous Mesoporous Mater.* **2003**, *60*, 19−30.
(28) Yazawa, T.; Machida, F.; Kubo, N.; Jin, T. Photocatalytic activity of transparent porous glass supported TiO2. *Ceram. Int.* **2009**, *35*, 3321−3325.

(29) Sakai, G.; Matsunaga, N.; Shimanoe, K.; Yamazoe, N. Theory of gas-diffusion controlled sensitivity for thin film semiconductor gas sensor. *Sens. Actuators, B* **2001**, *80*, 125−131.
(30) Shim, J. G.; Lee, D. W.; Lee, J. H.; Kwak, N. S. Experimental study on capture of carbon dioxide and production of sodium bicarbonate from sodium hydroxide. *Env. Eng. Res.* **2016**, *21*, 297−303.
(31) Tuguldurova, P. V.; Fateev, V. A.; Malkov, S. V.; Poleshchuk, K. O.; Vodyankina, V. O. Acetaldehyde-ammonia interaction: A DFT study of reaction mechanism and product identification. *J. Phys. Chem. A* **2017**, *121*, 3136−3141.
(32) Katada, N.; Niwa, M. Analysis of acidic properties of zeolitic and non-zeolitic solid acid catalysts using temperature-programmed desorption of ammonia. *Catal. Surv. Asia.* **2004**, *8*, 161−170.
(33) Setoyama, T.; Kobayashi, M.; Kabata, Y.; Kawai, T.; Nakanishi, A. New industrial process of PTMG catalyzed by solid acid. *Catal. Today* **2002**, *73*, 29−37.
(34) Flego, C.; Carluccio, L.; Rizzo, C.; Perego, C. Synthesis of mesoporous SiO_2−ZrO_2 mixed oxides by sol−gel method. *Catal. Commun.* **2001**, *2*, 43−48.
(35) Dickens, K. T.; Warren, S. *Chemistry of the carbonyl group: A step-by-step approach to understanding organic reaction mechanisms*; Willey: Iowa, 2018.
(36) Zonta, G.; Anania, G.; Fabbri, B.; Gaiardo, A.; Gherardi, S.; Giberti, A.; Guidi, V.; Landini, N.; Malagù, C. Detection of colorectal cancer biomarkers in the presence of interfering gases. *Sens. Actuators, B* **2015**, *218*, 289−295.
(37) Wang, C.; Hosomi, T.; Nagashima, K.; Takahashi, T.; Zhang, G.; Kanai, M.; Yoshida, H.; Yanagida, T. Phosphonic acid modified ZnO nanowire sensors: directing reaction pathway of volatile carbonyl compounds. *ACS Appl. Mater. Interfaces* **2020**, *12*, 44265−44272.
(38) Taleuzzaman, M. Limit of blank (LOB), limit of detection (LOD), and limit of quantification (LOQ). *Org. Med. Chem. I. J.* **2018**, *7*, 555722.
(39) Asanuma, K.; Hino, S.; Maruo, Y. Y. Development of an analytical chip for nitrogen monoxide detection using porous glass impregnated with 2-phenyl-4,4,5,5-tetramethylimidazoline-3-oxide-1-oxyl. *Microchem. J.* **2019**, *151*, No. 104251.
(40) Maruo, Y. Y.; Nakamura, M.; Higashijima, Y.; Kikuya, Y.; Nakamura, M. Development of highly sensitive nitrogen dioxide monitoring device and its application to wide-area ubiquitous network. *Sens. Actuators, B* **2012**, *173*, 191−196.

https://doi.org/10.1021/acsomega.2c07622
ACS Omega 2023, 8, 7874−7882